A pH Gated, Glucose-Sensitive Nanoparticle Based on Worm-Like Mesoporous Silica for Controlled Insulin Release

ARTICLE *in* THE JOURNAL OF PHYSICAL CHEMISTRY B · MARCH 2013

Impact Factor: 3.3 · DOI: 10.1021/jp400442x · Source: PubMed

5 AUTHORS, INCLUDING:

Lei Sun
Shandong University
51 PUBLICATIONS **242** CITATIONS
SEE PROFILE

Xinge Zhang
Nankai University
58 PUBLICATIONS **971** CITATIONS
SEE PROFILE

Chaoxing Li
Nankai University
55 PUBLICATIONS **864** CITATIONS
SEE PROFILE

THE JOURNAL OF PHYSICAL CHEMISTRY B

Article

pubs.acs.org/JPCB

A pH Gated, Glucose-Sensitive Nanoparticle Based on Worm-Like Mesoporous Silica for Controlled Insulin Release

Lei Sun,[†] Xinge Zhang,*[,†] Chao Zheng,[†] Zhongming Wu,[‡] and Chaoxing Li*[,†]

[†]Key Laboratory of Functional Polymer Materials of Ministry Education, Institute of Polymer Chemistry, Nankai University, Tianjin 300071, P. R. China

[‡]2011 Collaborative Innovation Center of Tianjin for Medical Epigenetics, Key Laboratory of Hormones and Development (Ministry of Health), Metabolic Diseases Hospital, Tianjin Medical University, Tianjin 300070, P. R. China

ABSTRACT: This study prepares a kind of core−shell hybrid nanoparticles, which is worm-like, pH gated, and glucose-sensitive. It has a mesoporous silica nanoparticle (MSN) core and polymer shell (cross-linked and non-cross-linked), bearing 3-acrylamidophenylboronic acid (AAPBA) and *N*-isopropylacrylamide (NIPAM) as sensor moieties. The shell of the nanoparticles has presented a distinct transition from swollen state to collapsed state as the temperature increases, which offers easy access to drug loading. Here, insulin is applied as a model drug and the behaviors of its loading/release are investigated. Insulin loading is up to 15% via mesoporous silica core. In vitro experiment shows that the cumulative release of insulin is dependent on glucose concentration, and the glucose sensitivity could be adjusted simply by different pH values. Simultaneously, compared with the non-cross-linked shell, the cross-linked shell, using dextran-maleic acid (Dex-Ma) as a macromolecule cross-link, enables insulin to release more persistently. Also, cell viability assay indicates that these nanoparticles have good biocompatibility. Consequently, the novel, pH gated, glucose-sensitive core−shell nanoparticles may have potential applications as a vehicle of self-regulated insulin delivery system.

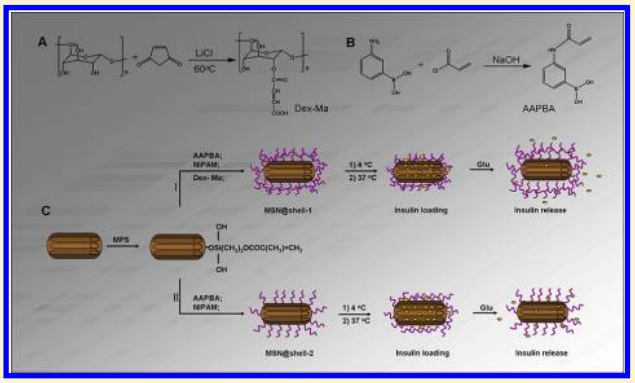

INTRODUCTION

Stimuli-responsive "smart" materials provide an attractive option for the design of self-regulated materials and systems. A number of stimuli types have been demonstrated to induce abrupt changes in the physicochemical properties of a polymer gel. In particular, chemical stimuli-responsive systems which can recognize fluctuations of specific molecules have attracted much attention due to their potential clinical applications.[1] One challenging molecule is glucose, since the metabolism of glucose in the body is significant and an unusual glucose level is a signal of disease such as diabetes. Actually, the treatment for insulin dependent diabetes mellitus conducted today is limited to insulin injection, which brings significant sufferings to patients. This situation has inspired a great deal of research to establish glucose-responsive systems for achieving self-regulated insulin delivery that can control the insulin dosage, avoiding overdose leading to serious hypoglycemia. Hence, to achieve this, phenylboronic acid may serve as a potential candidate for such a sensor. It can bind with saccharides containing *cis*-1,2- or *cis*-1,3-diols in aqueous medium, and exist in equilibrium between the uncharged and charged forms. Because the complex between the charged phenylborate and glucose itself is also anionically charged, the further addition of glucose induces a shift in the equilibrium to the direction of increasing the fraction of the charged forms, which makes it more hydrophilic.[2] It is also worth mentioning that the boronate ester bonds between saccharides and phenylboronic acids are sensitive to pH conditions.[3] Therefore, a pH gated glucose-responsive biomimetic insulin delivery system can be designed on the basis of the above properties of phenylboronic acids. What we need is to find a proper carrier for insulin loading. Mesoporous silica is a kind of such useful materials for the drug delivery system,[4] due to its large surface area,[5] large pore volume,[6] and ease of functionalization.[7] Mesoporous silica materials can load and protect therapeutic drugs and further control the release of preloaded drug molecules. Controlled release systems based on MSN have been achieved through several constructive strategies, such as surface functionalization with chemical groups to trigger drug release by a certain chemical mechanism,[8] capping mesopores with stimuli-removable nanoparticles,[9] and coating the outer shells of MSN with stimuli-responsive polymer layers.[10] Several research groups have studied the sustained-release properties of drugs loaded in conventional mesoporous silica microsized particles. Chang et al. proposed the coating of thermo- and pH-responsive polymer shell on magnetic mesoporous silica

Received: January 14, 2013
Revised: March 21, 2013
Published: March 21, 2013

Scheme 1. Schematic of Synthesis: (A) Dex-Ma; (B) AAPBA; (C) Core−Shell Nanoparticles and Insulin Loading/Release Based on Temperature and Glucose

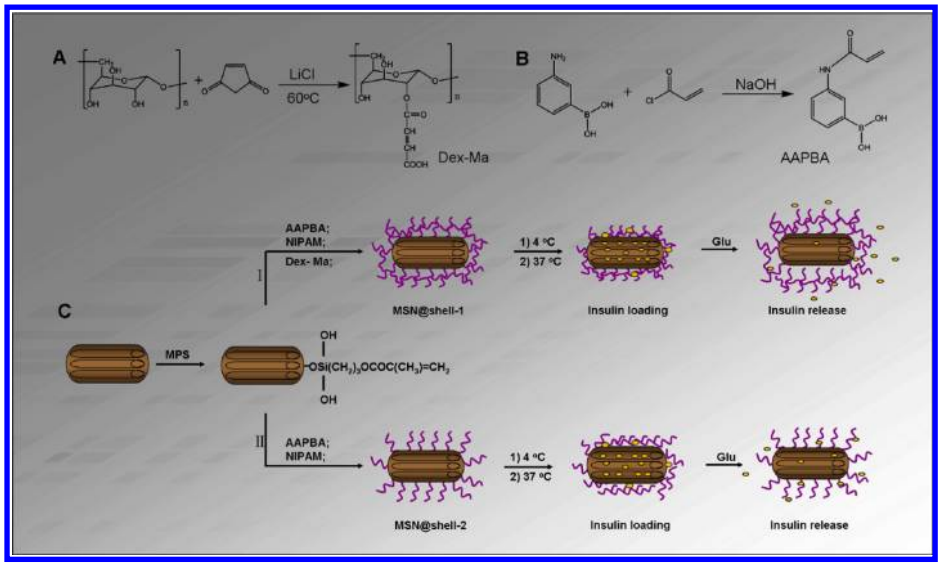

nanoparticles for controlled drug release.[11] Huang et al. reported the effect of the shape of mesoporous silica nanoparticles on cellular uptake and cell function, indicating that particles with larger aspect ratios are taken up in larger amounts and had faster internalization rates.[12] However, few have reported MSN-based insulin release systems. Tozuka et al. entrapped insulin into a group of folded-sheet mesoporous silica with different pore sizes and studied the in vitro release behaviors.[13] Zhao et al. demonstrated the glucose-triggered release of both gluconic acid-modified insulin (G-Ins) and cyclic adenosine monophosphate (cAMP) from MSN. G-Ins was immobilized on the exterior surface of MSN, serving as a gatekeeper to encapsulate cAMP inside the mesopores.[14] Zhao et al. reported a glucose-responsive controlled release of insulin system based on enzyme multilayer-coated mesoporous silica particles. The MSN serves as the drug reservoir, and the enzyme multilayers cross-linked with glutaraldehyde act as a valve to control insulin release in response to the external glucose level.[15] However, due to their antigenic nature, these protein-based components are intolerant of long-term use and storage. Furthermore, the glucose oxidase reactions often involve consumption of the analyte glucose, whose rates are inherently dependent on the dissolved oxygen, whereas concanavalin A evokes serious cytotoxicity and thus is hardly suitable for implantable applications.

Therefore, we combined the advantages of MSN with non-protein-based PBA derivatives and developed worm-like and pH gated glucose-sensitive core−shell hybrid nanoparticles. Here, the mesoporous core serves as the main reservoir for insulin, and the polymer shell (cross-linked and non-cross-linked), which bears 3-acrylamidophenylboronic acid (AAPBA), can be applied in insulin dosage at proper glucose and pH conditions. Thus, we investigated their swelling properties and insulin loading capacity and efficiency under different glucose concentrations, pH's, and temperatures. We also evaluated their insulin release behaviors triggered by different glucose concentrations, various saccharides at different pH conditions *in vitro*. Further, cell viability assay was also conducted under various concentrations of nanoparticles. The significance of this work lies in the high degree of controlling insulin release and in the potential applications of these core−shell nanoparticles in drug delivery systems.

EXPERIMENT

Materials. Cetyltrimethylammonium bromide (CTAB) and tetraethoxysilane (TEOS) were purchased from Kemiou Chemical Co. Ltd. (Tianjin, China). 3-(Methacryloxy)-porpyltrimethoxysilane (MPS) was available from Aldrich and distilled under a vacuum (CA, America). 3-Aminophenylboronic acid monohydrate was purchased from Nanjing Kangmanlin Chemical Industry Co. Ltd. (Nanjing, China). Maleic anhydride and ammonium persulfate (APS) were supplied by the Tianjin No. 2 Chemical Reagent Factory (Tianjin, China). Dextran (M_w 50 000) was purchased from ACROS Company (Beijing, China). *N*-Isopropylacrylamide (NIPAM) and lithium chloride were obtained from Aldrich Chemical Co (CA, America) and dried at 70 °C in a vacuum oven overnight. Acryloyl chloride was prepared by refluxing acrylic acid and thionyl chloride for 8 h at 90 °C in our laboratory and freshly distilled before use. All other reagents were of analytical grade and hadn't been further purified before used.

Synthesis of 3-(Methacryloxy)porpyltrimethoxysilane Modified Mesoporous Silica Nanoparticles (MPS-MSN). MPS-MSN were synthesized by condensation reaction under diluted TEOS and low surfactant conditions with $NH_3{\cdot}H_2O$ as a catalyst. Briefly, 0.1 g of CTAB was dissolved in 40 mL of H_2O, and 1 mL of $NH_3{\cdot}H_2O$ (30%) was added with stirring for 0.5 h. A 0.2 mL portion of TEOS was then added with vigorous stirring for 6 h at room temperature. Then, excess MPS (0.1 mL) was added to the above MSN under stirring and the mixture was stirred for another 12 h at room temperature.[16] The resultant nanoparticles containing templates were collected by centrifugation, and washed with distilled water/ethanol. The templates inside the MPS-MSN were removed by ion-exchange with NH_4NO_3/C_2H_5OH: 1.0 g of MPS-MSN powder was dispersed in 150 mL of ethanol containing 0.3 g of NH_4NO_3, refluxed at 60 °C for 8 h, centrifuged, washed three times with distilled water and ethanol, and then dried in a vacuum.

dx.doi.org/10.1021/jp400442x | J. Phys. Chem. B 2013, 117, 3852−3860

Synthesis of Dextran-Maleic Acid. The dextran-maleic acid was synthesized as previously reported.[17] As shown in Scheme 1A, dextran (445 mg) was dissolved in 20 mL of LiCl/DMF (10 wt %) solvent system at 90 °C under nitrogen gas. After dextran was clearly dissolved and cooled down to 60 °C, 0.032 mL of triethyamine was introduced to dextran solution as a catalyst, and the solution was stirred for 15 min. Maleic anhydride (2.205 g) was added to the reaction flask. The reaction was generally conducted for 8 h. The reaction product was precipitated with cold isopropyl alcohol, filtered, washed three times with isopropyl alcohol, and then dried at room temperature in a vacuum oven.

Synthesis of 3-Acrylamidophenylboronic Acid (AAPBA). AAPBA was synthesized as described by Shiomori et al.[18] As illustrated in Scheme 1B, 3-aminophenylboronic acid (7.44 g) was dissolved in 40 mL of sodium hydroxide (3.20 g) solution and cooled in an ice bath. Freshly distilled acryloyl chloride (3.2 mL) was added dropwise to the above solution under stirring. After cooling to room temperature, the reaction mixture was stirred for a further 2 h. The pH of the mixture was adjusted to pH 8 using dilute HCl (0.1 M). The resulting precipitate was filtered and washed by cold water several times. The precipitate was dissolved in 80 mL of distilled water heated to 80 °C, and the residual insoluble impurities were filtered off. The product was obtained by crystallization of the solution. The crystals were filtered, washed with cold distilled water, and dried in a vacuum oven.

Synthesis of MSN Nanoparticles Coated with Sensitive Polymer Shell. Monodisperse MSN@p(NIPAM-*co*-AAPBA-*co*-Dex-Ma) cross-linked core−shell nanoparticles (MSN@shell-1) were synthesized in the presence of MPS-MSN nanoparticles as seeds by the polymerization of NIPAM, AAPBA, and Dex-Ma with APS as initiator in water. Briefly, MPS-MSN nanoparticles, AAPBA, NIPAM, and Dex-Ma solutions were added into a 50 mL three-necked flask fitted with a reflux condensing tube. The reaction mixture was heated to 70 °C and bubbled with nitrogen gas for 1 h, and then, APS was added as an initiator. The reaction system was kept for another 8 h to allow the reaction to complete (Scheme 1CI). After the polymerization, the resultant MSN@shell-1 core−shell nanoparticles were purified by centrifugation and washed with distilled water three times.

Similarly, the non-cross-linked MSN@p(NIPAM-*co*-AAPBA) nanoparticles (MSN@shell-2) were synthesized by the same method as MSN@shell-1. The only difference was that Dex-Ma which served as a macromolecule cross-linking agent was not added (Scheme 1CII).

Characterization of Nanoparticles. The FT-IR spectra of samples were recorded in KBr pellets in a Fourier transform infrared spectrometer (Bio-Rad FTS-6000) in the range 4000−300 cm^{-1} for 32 scans. The hydrodynamic diameters and size distributions of nanoparticles were determined by dynamic light scattering (DLS) using a laser light scattering spectrometer (BI-200SM) equipped with a digital correlator (BI-9000AT). All samples were prepared from the suspension with a concentration of 10 $\mu g\ mL^{-1}$ after ultrasonic irradiation and then measured at different pH values, glucose concentrations, and temperatures, respectively. The hydrodynamic diameters (D_h) and the polydispersity indexes (PDI) were obtained by a cumulant analysis. The morphologies of nanoparticles were determined by transmission electron microscopy (TEM). Samples for TEM characterizations were dispersed in solvent, and a drop of the dispersion was spread onto the surface of a copper grid coated with a carbon membrane and then dried in a vacuum at room temperature for characterization. The thermogravimetric analyses of nanoparticles were conducted in nitrogen, at a heating rate of 10 °C min^{-1}, using a thermogravimetric analyzer (TGA; TG 209, NETZSCH). Real compositions of shells were tested by element analysis (vario EL CUBE).

Determination of Insulin Loading Capacity and Encapsulation Efficiency. MSN@shell nanoparticles (2.0 mg) were added to 5 mL of PBS (pH 8.5) containing insulin (0.5, 1.0, 2.0 mg) at 4 °C, and the mixtures were stirred for 48 h. Then, the temperature changed to 37 °C quickly; thus, the contractive shell kept insulin inside the nanoparticles. The entrapment efficiency (EE) and loading capacity (LC) of insulin were determined after isolation of the nanoparticles from the solution, which was achieved by three cycles of dispersion−centrifugation (17 000 × *g*, 30 min, 37 °C). The amount of free insulin in the collected supernatant was measured by the Bradford method using a UV spectrometer (Shimadzu UV-2550) at 595 nm.[19]

The EE and LC were calculated using the following equations:

$$\mathrm{EE\%} = \frac{\text{total insulin} - \text{free insulin}}{\text{total insulin}} \times 100\%$$

$$\mathrm{LC\%} = \frac{\text{total insulin} - \text{free insulin}}{\text{nanocomplexes weight}} \times 100\%$$

All measurements were performed in triplicate and averaged.

Insulin Release from MSN@shell Nanoparticles in Vitro. Insulin release from MSN@shell nanoparticles was analyzed by incubating nanoparticles in PBS with different glucose concentrations (0 and 5.0 mg mL^{-1}, pH 7.4) and different pH's (pH 6.3, 7.4, and 9.0) at 37 °C while shaking (100 rev min^{-1}). At predetermined time points, samples were centrifuged at 12 000 rpm for 5 min and the supernatants were taken and replenished by fresh PBS. The amount of free insulin was determined by the Bradford method, and a calibration curve was generated using blank nanoparticles to correct for the intrinsic absorption of the polymer. Samples were analyzed in triplicate with error bars representing the standard deviation.

Analysis of in Vitro Release Data. To determine the insulin release mechanism, the amount of released insulin versus time was studied using the following mathematical model:

$$M_t/M_\infty = kt^n$$

where M_t/M_∞ was the fractional amount of the insulin released at time t, k was a characteristic constant, and n was the release exponent, depending on the release mechanism and the geometry of the device. From the slope and intercept of the plot of $\log(M_t/M_\infty)$ vs $\log t$, kinetic parameters n and k were calculated. If Fickian diffusion occurred, n decreased to 0.5 for slab/cylinder/sphere. If non-Fickian (anomalous) diffusion dominated, the n value was between the above value corresponding to the polymer chain relaxation ($n < 1$) for slab/cylinder/sphere. Thus, through determination of the n value, the insulin release mechanism could be identified.[20]

Cell Viability. Cell viability was evaluated using A549 cells. The cell line was cultured in minimum essential medium (MEM) in a humidified atmosphere (5% CO_2/95% O_2). The cells were seeded into 96-well plates at 5000 cells per well. The plates were then returned to the incubator, and the cells were

dx.doi.org/10.1021/jp400442x | J. Phys. Chem. B 2013, 117, 3852−3860

Table 1. Size, Size Distribution, and Shell Thickness of MSN@shell Nanoparticles with Different Monomers

sample	MPS-MSN (mg)	AAPBA (mg)	Dex-Ma (mg)	NIPAM (mg)	APS (mg)	D_n[a] (nm)	PDI	shell thickness[b] (nm)
MSN@shell-1	20	15.0	35	70	4	265.0 ± 2.5	0.133	34.9 ± 1.3
MSN@shell-2	20	15.0		70	4	221.9 ± 3.2	0.214	14.7 ± 1.6
MPS-MSN						195.2 ± 4.1	0.034	

[a]D_n were obtained by DLS, 25 °C, pH 7.4. [b]Shell thickness was calculated from the relation: $(D_{\text{MSN-shell}} - D_{\text{MPS-MSN}})/2$, where $D_{\text{MSN-shell}}$ was the size of the nanoparticles and $D_{\text{MPS-MSN}}$ was the size of MPS-MSN.

allowed to grow to confluence for 24 h. Samples were dispersed in distilled water. The resulting suspensions were diluted with culture medium to give a final range of concentrations from 50 to 400 μg mL^{-1}. Then, the media in the wells were replaced with the readily prepared culture medium sample mixture (0.2 mL). The plates were returned to the incubator and maintained in 5% CO_2 at 37 °C for 24 and 48 h, respectively. Each sample was tested in three replicates per plate. After incubation culture medium, 0.2 mL of MTT solutions was used to replace the mixture in each well. Then, the plates were returned to the incubator and incubated for a further 4 h in 5% CO_2 at 37 °C. After the removal of culture medium and MTT, DMSO (0.15 mL) was added to each well to dissolve the formazane crystals. The optical density was read on a microplate reader at 490 nm. Cell viability was determined as a percentage of the negative control (untreated cells).[21]

Circular Dichroism Spectroscopy. The stability of the released insulin was determined by analysis of the conformation of released insulin using circular dichroism (CD), and the resulting spectrum was compared to standard insulin. The standard insulin solution was prepared in PBS (pH 7.4) to a final concentration of 0.05 mg mL^{-1}. CD measurements were performed on a Jasco J-715 CD spectropolarimeter at 25 °C with a cell length of 0.1 cm. For the far-UV CD spectra, samples were scanned from 190 to 260 nm and accumulated 10 times, at a resolution of 1.0 nm and a scanning speed of 100 nm min^{-1}.

RESULTS AND DISCUSSION

Synthesis of MSN@shell Nanoparticles. Nearly monodisperse MSN@shell-1 with cross-linked shell and MSN@shell-2 with non-cross-linked shell were prepared by the copolymerization of selected comonomers, as displayed in Table 1. The morphology of MPS-MSN was observed by TEM, as shown in Figure 1A, which indicated that MPS-MSN was a

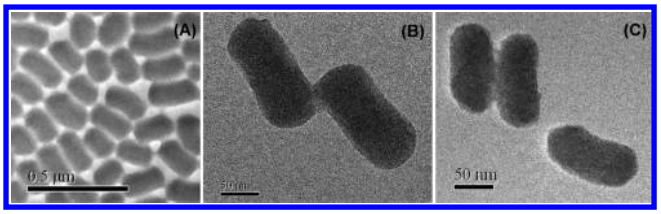

Figure 1. TEM micrographs: (A) MPS-MSN nanoparticles; (B) MSN@shell-1 nanoparticles; (C) MSN@shell-2 nanoparticles.

worm-like shape and a good monodispersity. The TEM micrographs of MSN@shell-1 (Figure 1B) and MSN@shell-2 (Figure 1C) indicated typical core–shell structure with a contrast of dark MSN core and light-colored shell layer. Moreover, both MSN@shell-1 and MSN@shell-2 represented relatively rough layers compared with the smooth surface of MPS-MSN because of the polymer shell. The cross-linked MSN@shell-1 exhibited a thicker shell than the non-cross-linked MSN@shell-2 in aqueous solution, as shown in Table 1.

Nitrogen adsorption–desorption measurements were conducted to characterize the mesoporous MPS-MSN nanoparticles, and the results are shown in Figure 2. The isotherms

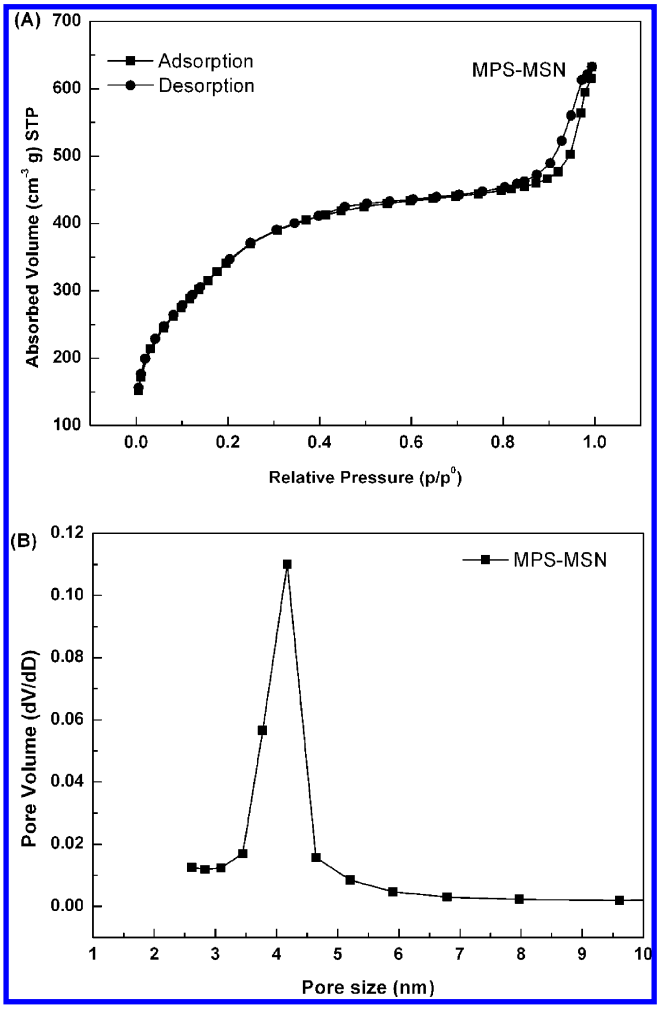

Figure 2. (A) Nitrogen adsorption–desorption isotherms of MPS-MSN nanoparticles. (B) Pore size distribution from adsorption branch.

of MPS-MSN nanoparticles exhibited the type IV isotherm characteristics, indicating the presence of well-defined mesopores. The Brunauer–Emmett–Teller (BET) surface area and pore volume of the MPS-MSN were 1279 m^2 g^{-1} and 0.87 cm^3 g^{-1}, respectively. The average pore size calculated from the adsorption branch of the nitrogen isotherms by the Barrett–Joiner–Halenda (BJH) method was 4.2 nm. Such a big pore size was available for insulin loading as the dimension of insulin was 3.3 × 2.7 × 2.5 nm^3.[22]

FT-IR spectra of MSN@shell-1 and MSN@shell-2 nanoparticles showed that the characteristic peak of the vinyl group

dx.doi.org/10.1021/jp400442x | J. Phys. Chem. B 2013, 117, 3852–3860

at 1630 cm^{-1} disappeared completely (Figure 3). The peaks between 2900 and 3000 cm^{-1} represented C−H vibration of

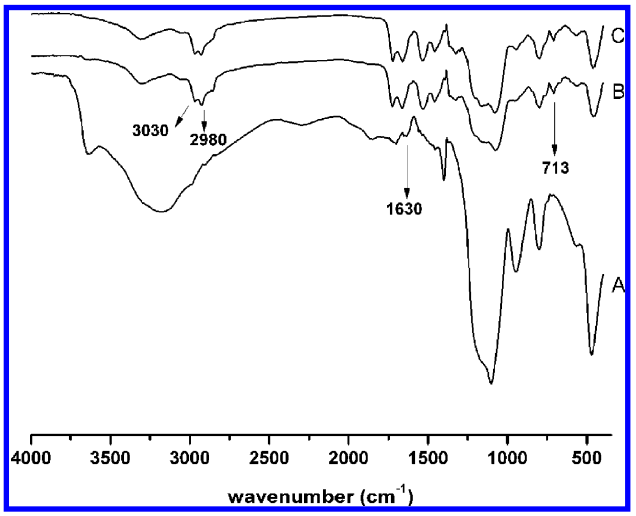

Figure 3. FT-IR spectra: (A) MPS-MSN; (B) MSN@shell-1; (C) MSN@shell-2.

methyl groups in NIPAM. The weak peak at 713 cm^{-1} was assigned to the out-of-plane bending vibration for the C−H group of m-substituted benzene in the AAPBA segment. Taken together, these results suggested the successful synthesis of MSN@shell nanoparticles.

Derivative thermo-gravimetric (DTG) and thermo-gravimetric (TG) curves for the MPS-MSN and MSN@shell nanoparticles were displayed in Figure 4. It was distinguishable from MPS-MSN and MSN@shell nanoparticles (Figure 4A). For MPS-MSN nanoparticles, it had a weight loss of 25% between 200 and 300 °C (Figure 4B), corresponding to the thermal decomposition of MPS components. This peak disappeared and performed two distinct degradations at around 100 and 410 °C in MSN@shell nanoparticles (Figure 4B). The first degradation, with a weight loss of 8%, was assigned to free water and water linked by hydrogen bonds, which was released at 25−135 °C and reached a maximum near 70 °C. The second degradation, occurring between 300 and 500 °C, displayed peaks with a maximum value at 410 °C and was assigned to the thermal degradation of the backbone.[23] At this stage, the decreases in MSN@shell-1 and MSN@shell-2 weight were approximately 63 and 57%, respectively.

Shell composition of microgels with different initial monomers was determined by element analysis. The result indicated that AAPBA content in MSN@shell-1 was 13.4% while that in MSN@shell-2 was 28.6%.

Multisensitivity of MSN@shell Nanoparticles. It was well-known that a hydrophilic/hydrophobic balance existed in poly(*N*-isopropylacrylamide) (pNIPAM) chains.[24] Low temperature favored hydrogen bonding interactions between amide groups and water molecules, which induced good solubility of pNIPAM. As the temperature increased, the hydrophilic/hydrophobic balance shifted to a more hydrophobic nature, resulting in the aggregation process. In addition, copolymerization of hydrophilic or hydrophobic monomers with NIPAM may greatly increase or decrease the lower critical solution temperature (LCST), which was probably caused by the change of hydrophilic/hydrophobic ratio.[25] As shown in Figure 5A, the size of MSN@shell-1 decreased considerably from 264 to 246

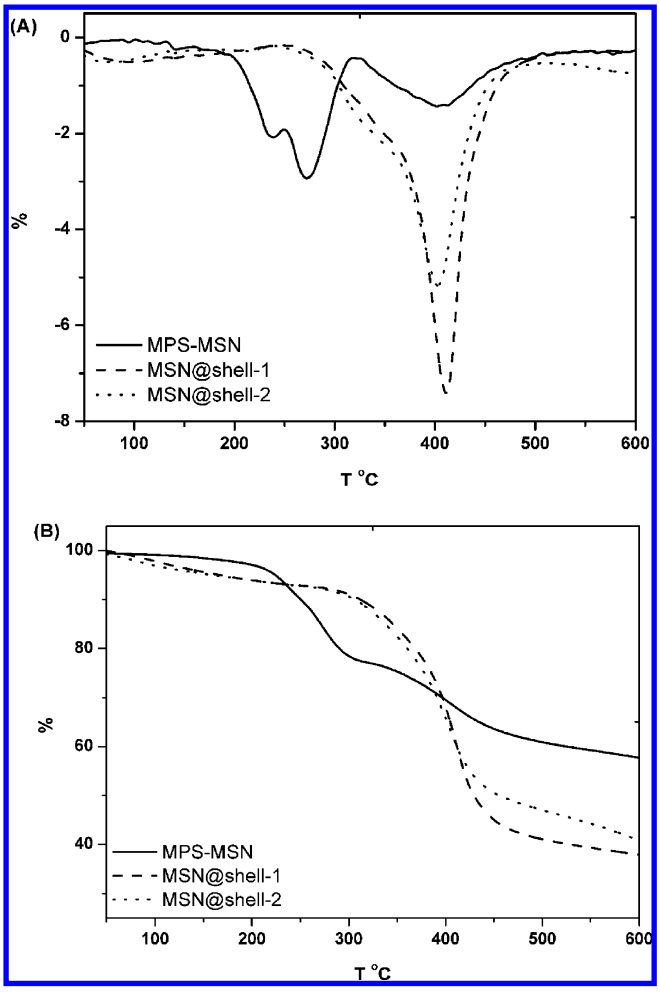

Figure 4. Thermal analysis of nanoparticles: (A) DTG; (B) TG.

nm when the temperature increased from 4 to 37 °C and the size of MSN@shell-2 decreased from 219 to 213 nm at the same condition. The results confirmed the thermo-responsive characteristics of the resultant nanoparticles and revealed a very good swelling−deswelling property. Additional studies focused on their glucose sensitivity. Figure 5A showed the change of nanoparticle sizes after the treatment of glucose at pH 7.4. The size of MSN@shell-1 increased considerably from 246 to 313 nm when the glucose concentration increased to 5.0 mg mL^{-1}. The size of MSN@shell-2 increased from 213 to 246 nm at the same conditions. It was because phenylboronic acid compounds in aqueous medium existed in equilibrium between uncharged and charged forms.[26] When the pH was near the pK_a of phenylboronic acid, the majority of phenylboronic acid existed in charged form, which facilitated the formation of a stable complex between charged phenylborate and glucose. Increasing the glucose concentration enhanced the charged phenylborates, thus increasing the hydrophilicity of the polymers, resulting in the increase of particle size. The pK_a could be conveniently adjusted by introducing a carboxyl group.[27] Such temperature and glucose sensitivities offered a convenient way for insulin loading and release. The sensitive selectivity of these core−shell nanoparticles was also studied. As we know, physiological fluids were composed of numerous substances which could potentially interact with the sensing segment. There were some other saccharides possessing *cis*-1,2- or *cis*-1,3-diols which may affect the sensitivity to glucose. The most abundant

dx.doi.org/10.1021/jp400442x | J. Phys. Chem. B 2013, 117, 3852−3860

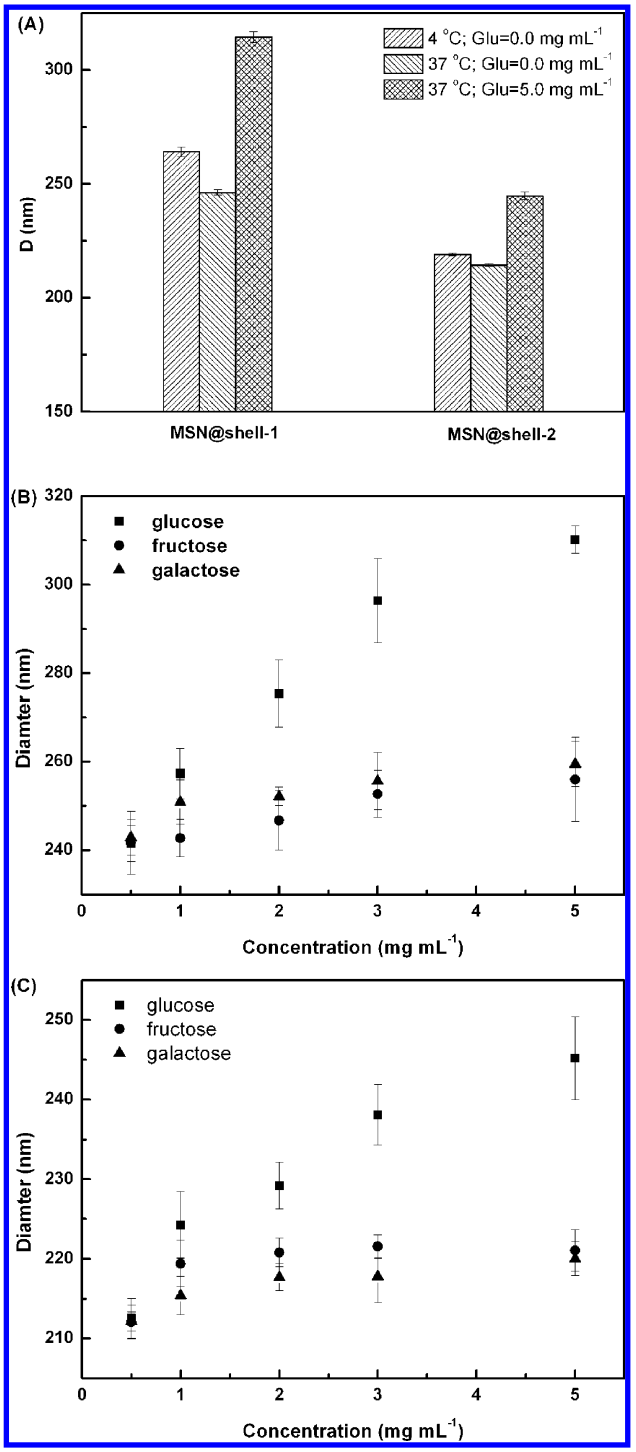

Figure 5. (A) Average hydrodynamic diameter of the nanoparticles under different temperatures and glucose concentrations, determined at pH 7.4 by DLS. Average hydrodynamic diameter of nanoparticles treated with different saccharides: (B) MSN@shell-1; (C) MSN@shell-2.

saccharides in blood after glucose were fructose and galactose. Although they were present at very minimal concentrations far lower than glucose (between 4 and 8 mM for healthy patients), the sensitivity of nanoparticles to them was worthy of study to prove the specificity selectivity for glucose. Figure 5B and C showed the diameter changes of core−shell nanopartices with different concentrations of glucose, galactose, and fructose. It was obvious that these phenyl-boronic acid modified nanoparticles showed a selective response to glucose with a diameter change of about 70 nm for MSN@shell-1 and 30 nm for MSN@shell-2, while the diameter changes were about 15 and 9 nm for galactose and fructose under the same concentration, respectively. The possible responsive mechanism we supposed was that phenylboronic acid could form a reversible cyclic ester with *cis*-diol moieties of saccharides in aqueous solution.[28] Glucose contains a pair of *cis*-diol units in the 1,2- and 5,6-positions. It was found that when two boronic acids possess the appropriate geometry they could selectively form a 2:1 complex with glucose, and only glucose had the required stereochemistry to create this complex, which led to glucose selectivity.[29] The other saccharides, fructose and galactose, could not form such complexes, so the diameter changes responding to fructose and galactose were not significant.

Insulin Loading and Release in Vitro. EE and LC of nanoparticles were shown in Table 2, which clearly indicated

Table 2. Insulin Loading Capacity (LC) and Encapsulation Efficiency (EE)

sample	insulin concentration (mg mL^{-1})	LC (%)	EE (%)
MSN@shell-1	0.5	11.3 ± 2.8	92.7 ± 5.6
	1.0	12.2 ± 3.6	81.2 ± 2.6
	2.0	15.0 ± 2.5	81.5 ± 5.0
MSN@shell-2	0.5	10.9 ± 5.6	93.8 ± 1.2
	1.0	11.3 ± 2.9	89.3 ± 9.2
	2.0	13.9 ± 2.6	87.4 ± 1.3

that EE and LC were affected by the initial concentration of insulin. As the concentration of insulin increased from 0.5 to 2.0 mg mL^{-1}, EE decreased to 80% slowly while LC increased to 15%, respectively. As shown in Table 2, both nanoparticles had high EE and LC, and these values corresponded closely to each other. What we could infer from this was that most insulin was encapsulated into MSN nanoparticles and shell contribution to EE and LC was not as much as MSN, that was to say, MSN nanoparticles played an important role in improving nanoparticle EE and LC.

Figure 6 showed the cumulative release of insulin from nanoparticles at 37 °C in different pH media at certain concentrations of glucose. Without glucose, both MSN@shell-1 and MSN@shell-2 emerged a rapid release and quickly reached release equilibrium about 10−15% within 5 h under different pH's (Figure 6A and C). We supposed that a small quantity of insulin was adsorbed onto the surface during the process of drug loading which led to a rapid diffusion when the nanoparticles came into release solution. However, MSN@shell-1 and MSN@shell-2 displayed different insulin release properties for 5.0 mg mL^{-1} of glucose. Take the case of MSN@shell-1. The amount of insulin release was around 20% at both pH 1.0 and 5.0, around 33% at pH 6.3, and 65 and 77% at pH 7.4 and 8.5, respectively, suggesting that insulin release from MSN@shell-1 depends on shell swelling. As just mentioned above, when the pH value was near the pK_a of phenylboronic acid, the majority of phenylboronic acid existed in charged form, which facilitated the formation of a stable complex between charged phenylborate and glucose. A relatively high concentration of glucose enhanced the charged phenylborates, thus increasing the hydrophilicity of the polymer shells, resulting in a swelling shell and leading to a considerable insulin release. MSN@shell-2 exhibited a very similar release

dx.doi.org/10.1021/jp400442x | J. Phys. Chem. B 2013, 117, 3852−3860

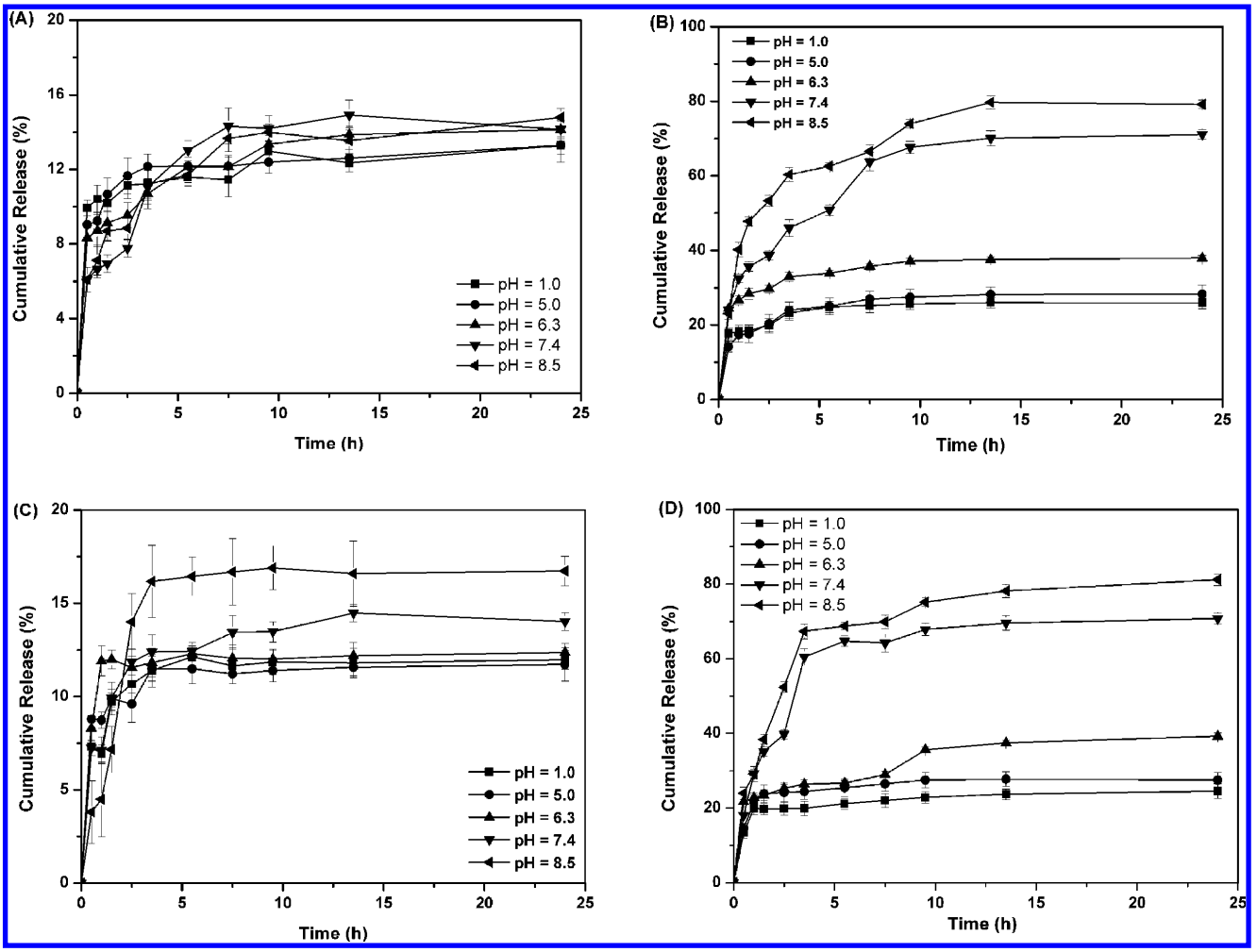

Figure 6. In vitro cumulative release of insulin: A and B for the MSN@shell-1 with glucose concentrations of 0 and 5.0 mg mL^{-1}, respectively; C and D for the MSN@shell-2 with glucose concentrations of 0 and 5.0 mg mL^{-1}, respectively.

Table 3. Drug Release Kinetic Data Obtained from Insulin Release Experiments

		Ridger–Peppas model			
sample	glucose concentration (mg mL^{-1})	n	k	R^2	transport mechanism
MSN@shell-1	0	0.3242	6.821	0.9169	diffusion controlled
	3	0.3152	30.90	0.9570	diffusion controlled
MSN@shell-2	0	0.1986	9.003264	0.9194	diffusion controlled
	3	0.3557	27.79073	0.92996	diffusion controlled

property that a low cumulative release percentage occurred at low pH while a remarkable large cumulative release percentage occurred at high pH. By contrast, MSN@shell-2 presented a fast release within 5 h (pH 7.4) and almost reached maximum release, while MSN@shell-1 exhibited a steady release until 10 h. Hence, we inferred that cross-linked and non-cross-linked shell structures had great influences on release rate especially at pH values near the pK_a of phenylboronic acid. Consequently, this pH affected glucose responsive system provided a novel sensing platform to recognize glucose through controlling environment stimulus and had potential applications for simulating the transport properties and controlled insulin release. In order to better study the release mechanism, the release data was analyzed according to the Ritger–Peppas equation. The results showed that R^2 was higher than 0.90 and n was lower than 0.5 in all cases (Table 3), indicating that insulin release was controlled by a drug diffusion process.

Biocompatibility Evaluation. Cells without the treatment of nanoparticles were taken as the control group, and the viability was set as 100%. The final report data were expressed as a percentage of the control group (mean standard deviation). The cytotoxicity of MSN@shell-1 and MSN@shell-2 nanoparticles was measured by MTT assay in the A549 cell line, which was an approach widely used to measure the mitochondria activity to quantify the cell growth or cell death.[30] The A549 cells were treated with the MSN@shell-1 and MSN@shell-2 samples at various concentrations (50, 100, 200, and 400 ug mL^{-1}) for 24 and 48 h (Figure 7). The toxicity was not observed even when the concentration was up to 400 ug mL^{-1}. It was interesting to note that the cell viability increased slightly as an increase of nanoparticles. Therefore, we confirmed that using MSN@shell-1 and MSN@shell-2 nanoparticles as the insulin carrier had the advantages of high drug

dx.doi.org/10.1021/jp400442x | J. Phys. Chem. B 2013, 117, 3852–3860

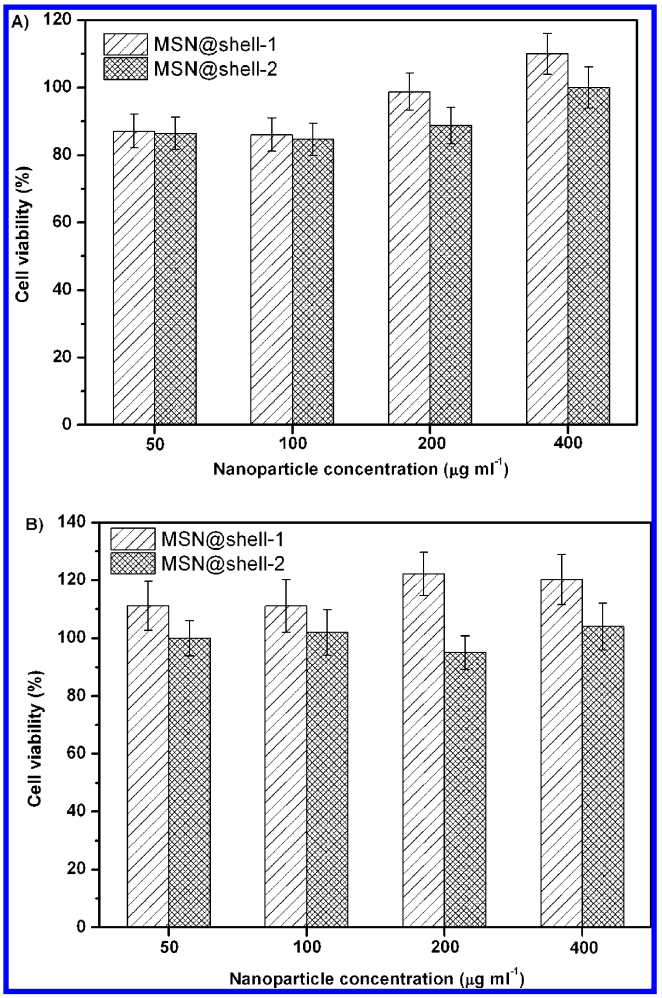

Figure 7. Cell viability of A549 cells after the treatment with MSN@shell-1 and MSN@shell-2 nanoparticles: (A) 24 h; (B) 48 h.

loading and good biocompatibility, which revealed the potential use for developing a smart insulin delivery system in vivo.

Circular Dichroism Spectra. Circular dichroism spectroscopy was used to examine the conformation and self-association of insulin.[31] The far-UV-CD band at 208 nm primarily arises from the α-helix structure, while that at 223 nm was for the β-structure. The ratio between both bands ([Φ]208/[Φ]223]) could be used to generate a qualitative measure of the overall conformational structure of insulin. In the present study, the [Φ]208/[Φ]223 ratio for standard insulin and released insulin was 1.23 and 1.14, respectively. As indicated by the CD spectrum (Figure 8), no significant conformational change was observed for the insulin released from the nanoparticles at pH 7.4 in comparison with the standard insulin. Furthermore, the spectral characteristics indicated that the tertiary structure of released insulin had not been distorted.

CONCLUSION

Here, worm-like multiresponsive cross-linked MSN@shell-1 and non-cross-linked MSN@shell-2 hybrid nanoparticles are successfully prepared by free radical polymerization. The hybrid nanoparticles display obviously thermo- and pH gated glucose sensitivity. The mesoporous core benefits the high insulin loading capacity, and temperature sensitivity provides a simple and effective way for insulin loading. The pH affecting glucose sensitivity offers a novel sensing platform to recognize glucose

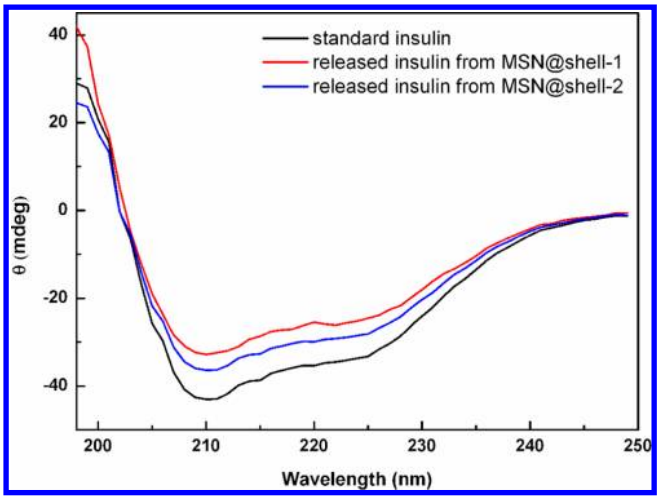

Figure 8. UV-CD spectra of standard insulin and released insulin.

through controlling environment stimulus. The cross-linked and non-cross-linked shell structures have great influences on release rate especially at pH near or over the pK_a of phenylboronic acid. Cell viability study indicates that these nanoparticles have good biocompatibility. Consequently, the novel pH gated, glucose-sensitive hybrid nanoparticles have potential applications for self-regulated insulin delivery systems.

AUTHOR INFORMATION

Corresponding Author

*Phone: +86-22-23501645. Fax: +86-22-23505598. E-mail: zhangxinge@nankai.edu.cn (X.Z.); lcx@nankai.edu.cn (C.L.).

Notes

The authors declare no competing financial interest.

ACKNOWLEDGMENTS

This work was supported by grants (81000683 to Z.W. and 51173085 to C.L.) from the National Natural Science Foundation of China.

REFERENCES

(1) Nakayama, D.; Takeoka, K. Y.; Watanabe.; Kataoka, K. Simple and Precise Preparation of a Porous Gel for a Colorimetric Glucose Sensor by a Templating Technique. *Angew. Chem., Int. Ed.* **2003**, *42*, 4197−4200.

(2) Liu, Y.; Deng, C. M.; Tang, L.; Qin, A. J.; Hu, R.; Sun, J. Z.; Tang, B. Z. Specific Detection of D-Glucose by a Tetraphenylethene-Based Fluorescent Sensor. *J. Am. Chem. Soc.* **2011**, *133*, 660−663.

(3) Xia, F.; Ge, H.; Hou, Y.; Sun, T.; Chen, L.; Zhang, G.; Jiang, L. Multiresponsive Surfaces Change between Superhydrophilicity and Superhydrophobicity. *Adv. Mater.* **2007**, *19*, 2520−2524.

(4) Lee, C. H.; Cheng, S. H.; Huang, I. P.; Souris, J. S.; Yang, C. S.; Mou, C. Y.; Lo, L. W. Intracellular pH-Responsive Mesoporous Silica Nanoparticles for the Controlled Release of Anticancer Chemotherapeutics. *Angew. Chem., Int. Ed.* **2010**, *49*, 8214−8219.

(5) Trewyn, B. G.; Giri, S.; Slowing, I. I.; Lin, V. S. Y. Mesoporous Silica Nanoparticle Based Controlled Release, Drug Delivery, and Biosensor Systems. *Chem. Commun.* **2007**, 3236−3245.

(6) Manzano, M.; Colilla, M.; Vallet-Regi, M. Drug Delivery from Ordered Mesoporous Matrices. *Expert Opin. Drug Delivery* **2009**, *6*, 1383−1400.

(7) Lei, C. H.; Liu, P.; Chen, B. W.; Mao, Y. M.; Engelmann, H.; Shin, Y. Local Release of Highly Loaded Antibodies from Functionalized Nanoporous Support for Cancer Immunotherapy. *J. Am. Chem. Soc.* **2010**, *132*, 6906−6907.

(8) Zhu, Y.; Shi, J.; Li, Y.; Chen, H.; Shen, W.; Dong, X. P. Storage and Release of Ibuprofen Drug Molecules in Hollow Mesoporous Silica Spheres with Modified Pore Surface. *Microporous Mesoporous Mater.* **2005**, *85*, 75−81.
(9) Ruiz-Hernandez, E.; Baeza, A.; Vallet-Regi, M. Smart Drug Delivery through DNA/ Magnetic Nanoparticle Gates. *ACS Nano* **2011**, *5*, 1259−1266.
(10) Liu, R.; Zhang, Y.; Feng, P. Multiresponsive Supramolecular Nanogated Ensembles. *J. Am. Chem. Soc.* **2009**, *131*, 15128−15129.
(11) Chang, B. S.; Sha, X. Y.; Guo, J.; Jiao, Y. F.; Wang, C. C.; Yang, W. L. Thermo and pH Dual Responsive, Polymer Shell Coated, Magnetic Mesoporous Silica Nanoparticles for Controlled Drug Release. *J. Mater. Chem.* **2011**, *21*, 9239−9247.
(12) Huang, X. L.; Teng, X.; Chen, D.; Tang, F. Q.; He, J. Q. The Effect of the Shape of Mesoporous Silica Nanoparticles on Cellular Uptake and Cell Function. *Biomaterials* **2010**, *31*, 438−448.
(13) Tozuka, Y.; ugiyama, S. E.; Takeuchi, H. Release Profile of Insulin Entrapped on Mesoporous Materials by Freeze−Thaw Method. *Int. J. Pharm.* **2010**, *386*, 172−177.
(14) Zhao, Y.; Trewyn, B. G.; Slowing, I. I.; Lin, V. S. Y. Mesoporous Silica Nanoparticle-Based Double Drug Delivery System for Glucose-Responsive Controlled Release of Insulin and Cyclic AMP. *J. Am. Chem. Soc.* **2009**, *131*, 8398−8400.
(15) Zhao, W. R.; Zhang, H. T.; He, Q. J.; Li, Y. S.; Gu, J. L.; Li, L. A Glucose-Responsive Controlled Release of Insulin System Based on Enzyme Multilayers-Coated Mesoporous Silica Particles. *Chem. Commun.* **2011**, *47*, 9459−9461.
(16) Huang, X. L.; Li, L. L.; Liu, T. L.; Hao, N. J.; Chen, D.; Tang, F. Q. The Shape Effect of Mesoporous Silica Nanoparticles on Biodistribution, Clearance, and Biocompatibility in Vivo. *ACS Nano* **2011**, *5*, 5390−5399.
(17) Kim, S. H.; Won, C. Y.; Chu, C. C. Synthesis and Characterization of Dextran-Maleic Acid Based Hydrogel. *J. Biomed. Mater. Res.* **1999**, *46*, 160−170.
(18) Shiomori, K.; Ivanov, A. E.; Galaev, I. Y.; Kawano, Y.; Mattiasson, B. Thermoresponsive Properties of Sugar Sensitive Copolymer of N-Isopropylacrylamide and 3-(Acrylamido)-phenylboronic Acid. *Macromol. Chem. Phys.* **2004**, *205*, 27−34.
(19) Yavuz, M. S.; Cheng, Y.; Chen, J.; Cobley, C. M.; Zhang, Q.; Rycenga, M. Gold Nanocages Covered by Smart Polymers for Controlled Release with near-Infrared Light. *Nat. Mater.* **2009**, *8*, 935−939.
(20) Nikolaos, A. Analysis of Fickian and Non-Fickian Drug Release from Polymers. *Pharm. Acta Helv.* **1985**, *60*, 110−111.
(21) Kwon, O. J.; Siegwart, D. J.; Lee, H. I.; Sherwood, G.; Peteanu, L.; Hollinger, J. O. Biodegradable Nanogels Prepared by Atom Transfer Radical Polymerization as Potential Drug Delivery Carriers: Synthesis, Biodegradation, in Vitro Release, and Bioconjugation. *J. Am. Chem. Soc.* **2007**, *129*, 5939−5945.
(22) Tsuboi, T.; McMahon, H. T.; Rutter, G. A. Mechanisms of Dense Core Vesicle Recapture Following "Kiss and Run" ("Cav-icapture") Exocytosis in Insulin-Secreting Cells. *J. Biol. Chem.* **2004**, *279*, 47115−47124.
(23) Zhou, W. J.; Naik, S. S.; Kurth, M. J.; Hsieh, Y. L.; Krochta, J. M. Synthesis and Characterization of Random Hydrophilic/Hydrophobic Copolymers of Styrene and D-Lactose-O-Vinylbenzylhydroxime. *J. Polym. Sci., Part A: Polym. Chem.* **1998**, *26*, 2971−2978.
(24) Zhang, X. Z.; Wu, D. Q.; Sun, G. M.; Chu, C. C. Novel Biodegradable and Thermosensitive Dex-AI/PNIPAAm Hydrogel. *Macromol. Biosci.* **2003**, *3*, 87−91.
(25) Stile, R. A.; Burghardt, W. R.; Healy, K. E. Synthesis and Characterization of Injectable Poly(N-isopropylacrylamide)-Based Hydrogels That Support Tissue Formation in Vitro. *Macromolecules* **1999**, *32*, 7370−7379.
(26) Matsumoto, A.; Yoshida, R.; Kataoka, K. Glucose-Responsive Polymer Gel Bearing Phenylborate Derivative as a Glucose-Sensing Moiety Operating at the Physiological pH. *Biomacromolecules* **2004**, *5*, 1038−1045.
(27) Matsumoto, A.; Yamamoto, K.; Yoshida, R.; Kataoka, K.; Aoyagi, T.; Miyahara, Y. A Totally Synthetic Glucose Responsive Gel Operating in Physiological Aqueous Conditions. *Chem. Commun.* **2010**, *46*, 2203−2205.
(28) Xia, F.; Ge, H.; Hou, Y.; Sun, T.; Chen, L.; Zhang, G.; Jiang, L. Multiresponsive Surfaces Change between Superhydrophilicity and Superhydrophobicity. *Adv. Mater.* **2007**, *19*, 2520−2524.
(29) Shimpuku, C.; Ozawa, R.; Sasaki, A.; Sato, F.; Hashimoto, T.; Yamauchi, A.; Suzuki, I.; Hayashita, T. Selective Glucose Recognition by Boronic Acid Azoprobe/c-Cyclodextrin Complexes in Water. *Chem. Commun.* **2009**, 1709−1711.
(30) Chang, J. S.; Chang, K. L. B.; Hwang, D. F.; Kong, Z. L. In Vitro Cytotoxicitiy of Silica Nanoparticles at High Concentrations Strongly Depends on the Metabolic Activity Type of the Cell Line. *Environ. Sci. Technol.* **2007**, *41*, 2064−2068.
(31) Lee, S.; Kim, K.; Kumar, T. S.; Lee, J.; Kim, S. K.; Lee, D. Y. Synthesis and Biological Properties of Insulin−Deoxycholic Acid Chemical Conjugates. *Bioconjugate Chem.* **2005**, *16*, 615−620.